International Journal of the Physical Sciences Vol. 6(31), pp. 7212 - 7221, 30 November, 2011
Available online at http://www.academicjournals.org/IJPS
DOI: 10.5897/IJPS11.832
ISSN 1992 - 1950 ©2011 Academic Journals

Full Length Research Paper

The study of specific absorption rate (SAR) reduction in mobile phones using materials and metamaterials

Mohammad Rashed Iqbal Faruque[1,2]*, Mohammad Tariqul Islam[1] and Norbahiah Misran[1,2]

[1]Institute of Space Science (ANGKASA), Universiti Kebangsaan Malaysia, 43600 UKM, Bangi, Selangor, Malaysia.
[2]Department of Electrical, Electronic and Systems Engineering, Faculty of Engineering and Built Environment, Universiti Kebangsaan Malaysia, 43600 UKM, Bangi, Selangor, Malaysia.

Accepted 1 September, 2011

In this paper, reducing of specific absorption rate (SAR) with materials and metamaterials attachment is investigated. The finite-difference time-domain method with lossy-Drude model is adopted in this study. The methodology of SAR reduction is addressed and the belongings of attaching position, distance, and size of ferrite sheet material properties, perfect electric conductor (PEC), and metamaterials on the SAR reduction are investigated. Materials have achieved a 47.02% reduction of the initial SAR value while metamaterials achieved a reduction of 49.21% respectively for the case of 1 g SAR. These results propose a guideline to decide assorted types of materials and metamaterials with the utmost SAR reducing effect for a phone model.

Key words: Antenna, human head model, lossy-Drude model, materials, metamaterials, specific absorption rate (SAR), symmetry.

INTRODUCTION

Sources of radio frequency/microwave (RF/MW) radiation, particularly cellular phones are ever present. RF/MW sources are part of daily life, but they also reason for concern regarding the possible biological effects of microwaves. It is important that the biological effects of RF/MW fields be minimal, at least at the level of their clinical significance, so that health risk can be assessed. Because the potential shock of RF/MW fields on human health has not yet been well characterized; the basic knowledge from laboratory studies based on cellular and animal test systems are invaluable. The Interaction of handset antennas with the human body is a great consideration in cellular communications. The user's body, especially the head and hand, influence the antenna voltage standing wave ratio (VSWR), gain, and radiation patterns. Furthermore, thermal effects, when tissues are exposed to unlimited electromagnetic energy, can be a serious health hazard. Therefore standards organizations have set exposure limits in terms of specific absorption rate (SAR) (IEEE C95.1-2005, 2005; International Non-Ionizing Radiation Committee of the International Radiation Protection Association, 1988). SAR is a measure of the rate at which radio frequency (RF) energy is immersed by the body when bared to a radio-frequency electro-magnetic field. SAR is used to quantify exposure to fields among 100 kHz and 10 GHz (Hirata et al., 2004; Chan et al., 2005; Erentok et al., 2005). It is frequently used to quantify power immersed from cellular phones and through MRI scans. The importance will depend on the geometry of the element of the body that is bared to the RF energy and on the exact position and geometry of the RF source.

Cellular phone protection and the enforcement of pertinent exposure standards are issues in the current media, and regulatory agencies are motivated to assure that compliance testing is acceptable. IEEE Standard 1528 (IEEE C95.1-2005) and IEC 62209-1 specify protocols and process for the measurement of the peak spatial-average SAR induced inside a simplified model of the head of users of hand held radio transceivers (cellular phones). For example, the SAR limit specified in IEEE C95.1: 1999 is 1.6 W/kg in a SAR 1 g averaging mass while that specified in IEEE C95.1: 2005 has been up-dated to 2 W/kg in a 10 g averaging mass (International Non-Ionizing Radiation Committee of the International Radiation Protection Association, 1988). This new SAR

*Corresponding author. E-mail: rashedgen@yahoo.com.

limit specified in IEEE C95.1: 2005 is comparable to the limit specified in the International Commission on Non-Ionizing Radiation Protection (ICNIRP) guidelines.

The interaction of the cellular handset with the human head has been investigated by many published papers considering; first, the effect of the human head on the handset antenna performance including the feed-point impedance, gain, and efficiency (Hirata et al., 2004; Chan et al., 2005; Erentok et al., 2005; Fung et al., 2002; Wang and Fujiwara, 1999; Curto et al., 2009; Wang and Fujiwara, 1997; Kiminami et al., 2008; Islam et al., 2009), and second, the impact of the antenna EM radiation on the user's head due to the absorbed power, which is measured by predicting the induced SAR in the head tissue (Kiminami et al., 2008; Islam et al., 2009; Li et al., 2009; Kiverkas et al., 2004; Hawang and Chen, 2006).

The most used method to solve the electromagnetic problem in this area is the finite-difference time-domain (FDTD) technique (Kiverkas et al., 2004; Hawang and Chen, 2006; Faruque et al., 2010a, b; Islam et al., 2010a, b). Specifically, the problems to be solved in SAR reduction need a correct representation of the cellular phone, anatomical representation of the head, alignment of the phone and the head, and suitable design of materials or metamaterials.

In Wang and Fujiwara, (1997), a ferrite sheet was adopted as safety among the antenna and the human head. A reduction of above 13% for the spatial peak SAR over 1 g averaging was attained. A study on the belongings of attaching a ferrite sheet for SAR reduction was presented in Pendry et al. (1999), and it was completed that the position of protecting plays a vital role in the reduction effectiveness.

In Kuo and Kuo, (2003), for the SAR in the human head, an effective approach is the use of a planar antenna integrated onto the back side (away from the head) of a phone model, but it carries additional design difficulties above all in achieving the required frequency bandwidth and radiation efficiency. Another come up to is the use of a directional or reflecting antenna (Pendry et al., 1999; Smith et al., 2000; Pederson and Andersen, 1994; Tay et al., 1998; Misran et al., 2011). Such an antenna structure sacrifices the availability of signals received from all directions to the phone model. The method of SAR reduction by ferrite sheet attachment was due to the repression of surface currents on the frontage of phone model (Tay et al., 1998; Fung et al., 2003). However, the association between the utmost SAR reducing outcome and the parameters such as attaching position, size and material properties of ferrite material remains unknown.

Metamaterials have inspired great interest due to their unique physical properties and novel application (Hawang and Chen, 2006; Ziolkowski, 2003; Faruque et al 2011a, b, c, d, e, f). Metamaterials denote artificially constructed materials having electromagnetic properties not generally found in nature. Two important parameters, electric permittivity and magnetic permeability determine the response of the materials and metamaterials to electromagnetic fields. The negative permittivity can be obtained by arranging the metallic thin wires periodically (Smith and Kroll, 2000; Beard et al., 2006; Sigalalas et al., 2001). On the other hand, an array of split ring resonators (SRRS) can exhibit negative effective permeability. The designed SRRS operated at 1.8 GHz and were used to reduce the SAR value in a lossy material.

At first, materials are placed between the antenna and a human head, and then replaced by a metamaterial. In order to study the SAR reduction of an antenna operated at the GSM 900 band, the effective medium parameter of metamaterials is set to be negative at 900 MHz (Sigalalas et al., 2001). Different positions, sizes, and negative medium parameters of material and metamaterials for SAR reduction effectiveness are also analyzed.

SIMULATION MODEL AND NUMERICAL TECHNIQUES

The simulation model which includes the handset with PIFA type of antenna and the SAM phantom head provided by CST Microwave Studio® (CST MWS) is considered in this paper. A complete handset model composed of the circuit board, LCD display, keypad, battery, and housing was used for simulation. The relative permittivity and conductivity of individual components were set to comply with industrial standards. In addition, definitions in Hirata et al. (2004), Chan et al. (2005), Kuo and Kuo (2003), and Islam et al. (2011a, b) were adopted for material parameters involved in the SAM phantom head. In order to precisely characterize the performance over a broad frequency range, dispersive models for all the dielectrics were adopted during the simulation (Hirata et al., 2004; Islam et al., 2009). A PIFA antenna constructed in a helical sense operating at 900 MHz for GSM application was used in the simulation model. In order to obtain a high-quality geometry approximation for such a helical structure, a predictable meshing scheme was used in the FDTD method (Islam et al., 2010a). Usually, it requires huge number of hexahedrons which in turn makes it extremely demanding to get convergent results within sensible simulation time.

Figure 1 shows a moveable telephone model at 900 MHz for the current study. It was calculated to be a quarter wavelength PIFA antenna mounted on a rectangular conducting box. The conducting box was 10 cm tall, 4 cm wide and 3 cm thick. The PIFA antenna was located at the top surface of the conducting box. A space domain enclosing the human head and the phone model is also shown in Figure 1. The time-stepping was performed for about eight sinusoidal cycles in order to reach a steady state. To absorb the outgoing scattered waves, the second order Mur absorbing boundaries acting on electric fields were used.

The head models used in this study were obtained from a MRI-based head model through the whole brain Atlas website. Six types of tissues, that is, bone, brain, muscle, eye ball, fat, and skin were involved in this model (Ziolkowski, 2003; Smith et al., 2000; Faruque et al., 2010a). The dielectric properties of these tissues are shown in Table 1.

IMPACT ON SAR OF FERRITE SHEET ATTACHMENT

Here, a ferrite sheet is placed between the antenna and a human head thus reducing the SAR value. In order to study SAR reduction of an antenna operated at the GSM 900 band, different positions, sizes, and ferrite sheet materials for SAR reduction effectiveness are also analyzed by using the FDTD method in conjunction with a

Table 1. Dielectric tissue properties at 900 MHz.

Material	Density, ρ (Kg-m $^{-3}$)	Conductivity, σ (S-m $^{-1}$)	Relative permittivity ε_r
Fat, bone	1130	0.12	4.83
Muscle, skin	1020	1.5	50.5
Brain	1050	1.11	41.7
Eye ball	1000	2.03	68.6

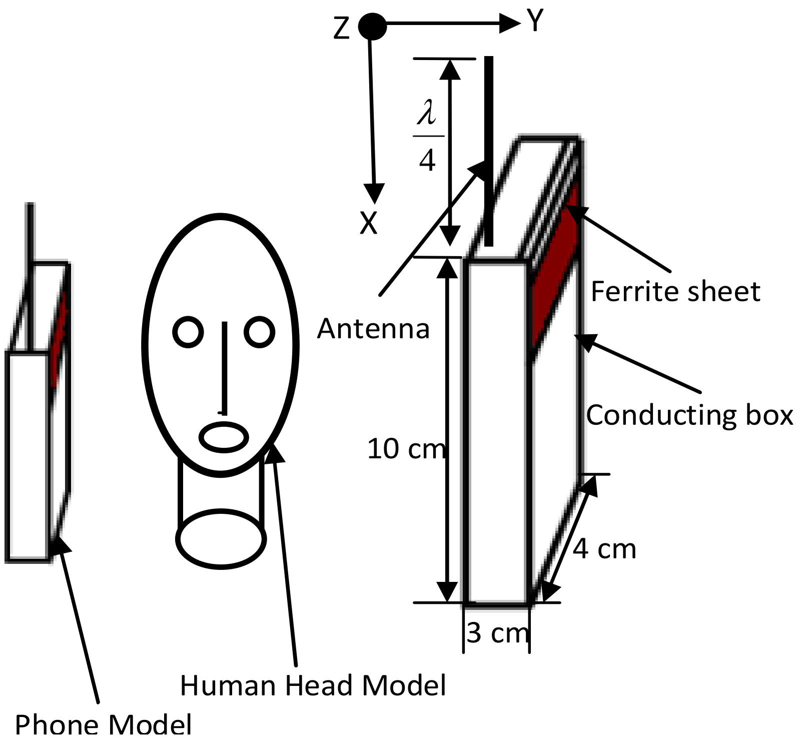

Figure 1. Models of the head and portable telephone with an attached ferrite sheet.

detailed human head model.

The dispersive models for all the dielectrics were adopted during the simulation in order to accurately characterize the ferrite sheet. The antenna was arranged in parallel to the head axis, the distance is varied from 5 to 20 mm, and finally 20 mm was chosen for comparison with the ferrite sheet. Besides that, the output power of the mobile phone model needs to be set before SAR is simulated. In this paper, the output power of the cellular phone is 500 mW at the operating frequency of 900 MHz. In the real case, the output power of the mobile phone will not exceed 250 mW for normal use, while the maximum output power can reach to 1 W or 2 W when the base station is far away from the mobile station (cellular phone). The SAR simulation is compared with the results in Wang and Fujiwara (1999) and Kuo and Kuo (2003) for validation, as shown in Table 2. The calculated peak SAR 1 g value is 2.002 W/kg, and SAR 10 g value is 1.293 W/kg when the phone model is placed 20 mm away from the human head model without a ferrite sheet. This SAR value is better compared with the result reported in Hawang and Chen (2006), which is 2.43 W/kg for SAR 1 g. The ferrite sheet material is utilized in between the phone and head models, and it is found that the simulated value of SAR 1 and 10 g are 1.043 and 0.676 W/kg, respectively. The reduction of about 47.02% was observed in this study when a ferrite sheet is attached between the phone and human head models for SAR 1 g. This SAR reduction is better than the result reported in Wang and Fujiwara, (1997), which is 13% for SAR 1 g. This is achieved using different radiating powers and impedance factors. Figures 2 to 3 show the SAR value compared with the distance between phone and head models, without and with of ferrite sheet respectively.

Table 2. Comparisons of peak SAR with ferrite sheet attachment.

Tissue	SAR value (W/kg)
SAR value for (Wang and Fujiwara, 1999)	2.17
SAR value for (Kuo and Kuo, 2003)	2.28
SAR value with ferrite sheet for 1 gm	1.043

The reduction efficiency of the SAR depends on its width and height. In order to definitely confirm this 1 and 10 g average, was SAR compared with the width, thickness, and height of ferrite sheet

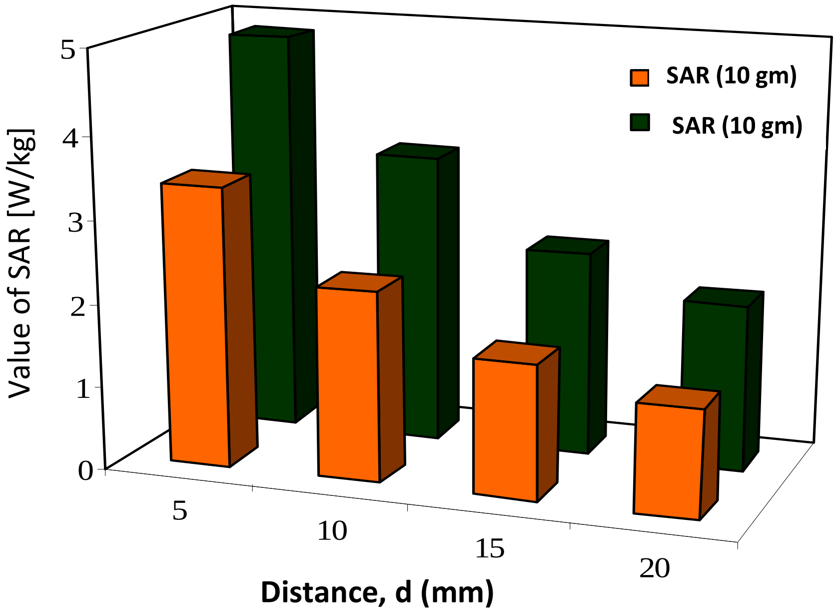

Figure 2. SAR value compared with the distance among phone model and human head model without ferrite sheet.

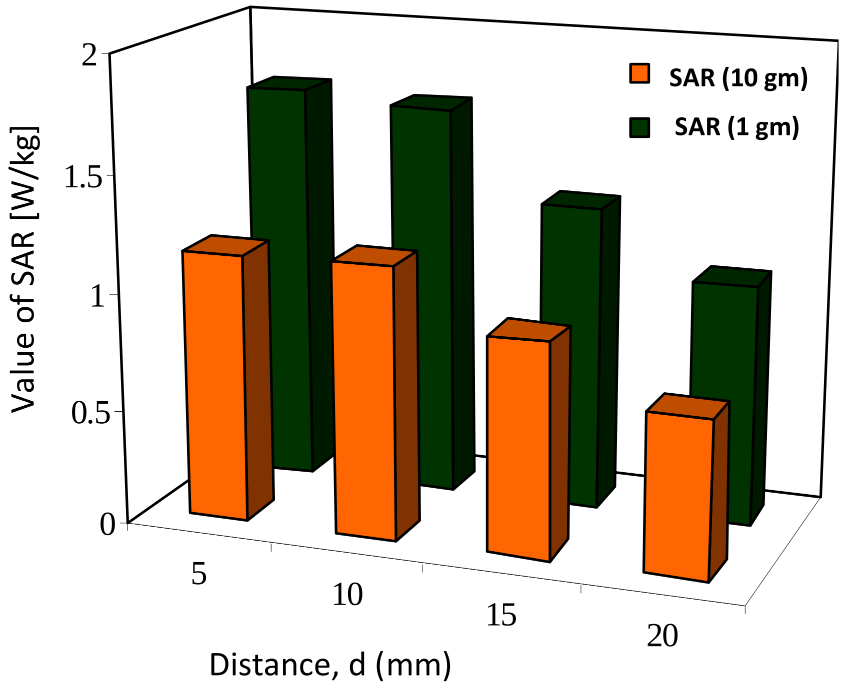

Figure 3. SAR value compared with the distance among phone model and human head model with ferrite sheet.

described in previous published paper (Islam et al., 2009). In Figure 2, it is shown that if the distance between phone and human head models is varied then the SAR value decreases. This is because the dielectric constant, conductivity, density and magnetic tangent losses are also varied. In (Islam et al., 2009), it was observed that the SAR value reduces with the increase of the width of the ferrite sheet. As shown in this paper, the SAR value was decreases until a thickness of 3 mm, and then a different tendency that is, it started to increase after 3 mm. Also the height of the ferrite sheet was varied up to 90 mm. It was shown that if the height of the ferrite sheet increases, then the SAR value also decreases up to a height of 80 mm, and it started to increase after 80 mm. Figure 3 shows the SAR value with ferrite sheet attachment for 1 and 10 g average SAR. It can be observed that with ferrite sheet attachment, the SAR value has been decreased for the case of 1 and 10 g average SAR. The results implies that only suppressing the maximum current on the front side of the conducting box contributes significantly to the reduction of spatial peak SAR. This is because the decreased quantity of the power absorbed in the head is considerably larger than that dissipated in the ferrite sheet.

REDUCTION OF SAR USING METAMATERIAL

SAR in the head can be reduced by placing a metamaterial among the antenna and the human head. The metamaterial is on a scale less than the operating wavelength. The structures are resonant due to internal capacitance and inductance. The stop band can be designed at the operation bands of cellular phone radiation. The metamaterial are designed on a printed circuit board so it may be easily integrated to the cellular phone. By arranging sub-wavelength resonators periodically we get the metamaterial structure.

SRRS structure

We establish that metamaterials can be used to reduce the peak SAR 1 g and SAR 10 g in the head from the FDTD analysis. Here, metamaterials operated at the 900 and 1800 MHz bands of the cellular phone were considered. The metamaterials can be attained by arranging SRRS periodically. The SRRS structure consists of two concentric rings of conductive material. There is a gap on every ring, and every ring is positioned opposite to the gap on the additional ring. The schematics of the SRRS structure that we used in this study as shown in Figure 4. The significant frequency of the SRRS can be varied toward a higher or lower frequency band by appropriately choosing these structure parameters.

SRRS design

To construct the metamaterial for SAR reduction, we proposed one model of resonators namely the SRRS as shown in Figure 4. We design the resonators for operation at the 900 MHz bands. The SRRS contains two square rings, each with gaps appearing on the opposite sides (Hawang and Chen, 2006). The SRRS was introduced by Pendry et al. (1999) and subsequently used by Smith et al. for synthesis of the first left-handed artificial medium (Ziolkowski, 2003). A lot of effort worldwide has been spent studying single negative metamaterials (SNMs), double negative metamaterials (DNMs), their properties (Hirata et al., 2004; Chan et al., 2005; Erentok et al., 2005; Ziolkowski, 2003), applications in antennas (Erentok et al., 2005; Ziolkowski, 2003; Smith and Kroll, 2000), and other microwave devices (Ziolkowski, 2003; Smith and Kroll, 2000; Beard et al., 2006). In Figure 4, the structures of resonators are defined by the following structure parameters: The ring thickness *c*, the ring gap *d*, the square ring size *l*, the split gap *g,* and c_0 is the speed of light in free space. The resonant frequency *f* is very sensitive to small changes in the structure dimensions of the SRRS. The frequency response can be scaled to higher or lower frequency by properly choosing these geometry parameters. After an extensive simulation study, we have found out a closed-form formula for the resonant frequencies of the SRRS:

$$f_{SRRS} = k_1 \frac{c_0}{2[4(2r_{ext} - c) - g]\varepsilon_r^{1/2}} \quad (1)$$

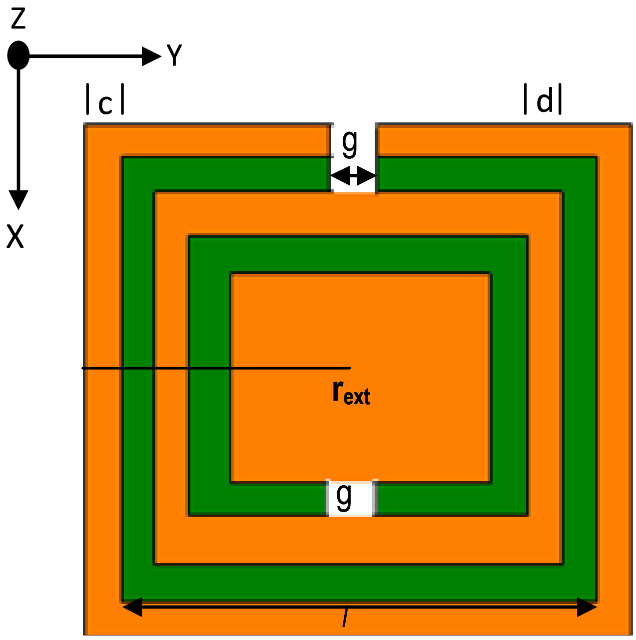

Figure 4. The structure of the SRRS used in this calculation.

The SRRS is resonating at approximately half the guided-wavelength of the resonant frequency. There are two resonances from the split rings. We have given the formula for the resonance of the outer split ring, which has a lower resonance frequency.

Numerical simulations that predict the transmission properties depend on the various structure parameters of this system. Simulations of this complex structure are performed with the FDTD method. To construct the resonators for SAR reduction, let us assume that the resonators lie in the *xz* plane, as shown in Figure 5. The EM wave propagates along the *y* direction. The electric polarization is kept along the *z*-axis and magnetic field polarization is kept along *x* axis. Periodic boundary conditions are used to reduce the computational domain and an absorbing boundary condition is used at the propagation regions. The total-field/scatter-field formulation is used to excite the plane wave. The regions inside of the computational domain and outside of the SRRS were assumed to be vacuums.

From this study, it is found that both incident polarizations can produce a stop band. As shown in Beard et al. (2006), Sigalalas et al. (2001) and Coccioli et al. (1999); the stop band corresponds to a region where either the permittivity or permeability is negative. When the magnetic field is polarized along the split ring axes, it will produce a magnetic field that may either oppose or enhance the incident field. A large capacitance in the region between the rings will be generated and the electric field will be powerfully concentrated. There is strong field coupling between the SRRS and the permeability of the medium will be negative at the stop band. Because the magnetic field is parallel to the plane of SRRS, we imagine the magnetic effects are small, and that permeability is small, positive, and slowly varying. In this condition, these structures can be viewed as arranging the metallic wires periodically.

The stop bands of the SRRS are designed to be at 900 and 1800 MHz. The periodicity along *x*, *y*, *z* axes are L_x = 63 mm, L_y = 1.5 mm, and L_z = 63 mm, respectively. On the other hand, to obtain a stop band at 1800 MHz, the parameters of the SRRS are chosen as *c* = 1.8 mm, *d* = 0.6 mm, *g* = 0.6 mm, and *r* = 12.9 mm. The periodicity along the *x*, *y*, *z* axes are L_x = 50 mm, L_y = 1.5 mm, and

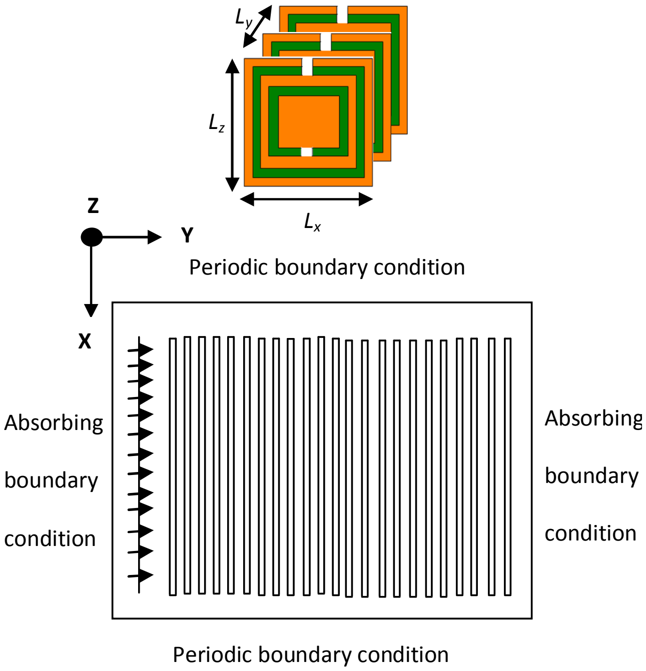

Figure 5. Top view of an incident plane wave on the periodic SRRS.

L_z = 50 mm, respectively. Both the thickness and dielectric constant of the circuit boards for 900 and 1800 MHz are 0.508 and 3.38 mm, respectively. After properly choosing geometry parameters, the SRRS medium can display a stop band around 900 and 1800 MHz. The SRRS producing a good stop band and size are large. Therefore, SRRS are suitable for mobile phones as per size and recital point of view.

We have tried to use a high impedance surface configuration (Smith and Kroll, 2000) to reduce the peak SAR. However, we found that when these structures operate at 900 MHz, the sizes of these structures are too large for cellular phone application. A negative permittivity medium can also be constructed by arranging the metallic thin wires periodically (Sigalalas et al., 2001). However, we found that when the thin wires operate at 900 MHz, the size is also too large for practical application. Because the SRRS structures are significant due to internal capacitance and inductance, they are on a scale less than the wavelength of radiation. In this study, it is established that the SRRS can be designed at 900 MHz while the size is similar to that of a cellular phone.

RESULTS AND DISCUSSION

The designed SRRS were placed between the antenna and the human head. The antenna was arranged parallel to the head axis. The distance between the antenna and head surface was 20 mm. The SAR value was calculated for an antenna output power equal to 600 mW. The calculated peak SAR 1 g without metamaterials was 2.002 W/kg. The SAR simulation is compared with the results in Wang and Fujiwara (1999) and Kuo and Kuo (2003) for validation, as shown in Table 2. The distance between the antenna feeding point and edge of the metamaterials was A= 3 mm. The size of the metamaterials in the *xz* plane was 48 × 48 mm and the thickness was 6 mm. The SAR value and antenna performance with the metamaterial were analyzed. To evaluate the power radiated from the antenna, the source impedance (Z_S) was assumed to be equal to the complex conjugate of the free space radiation impedance (Z_S = 102.14+ j83.78 Ω). The source voltage (V_S) was chosen to obtain a radiated power in free space equal to 600 mW (V_S = $\sqrt{0.6.8.R_{R0}}$.). When analyzing the effect of the metamaterials and the human head on the antenna performance, the source impedance and source voltage were fixed at the Z_S and V_S values. The power radiated from the antenna was evaluated by comparing the radiation impedance in this situation (Z_R= R_R+ jX_R) and used the following (Tay et al., 1998) equation:

$$P_R = \frac{1}{2} V_S^{\,2} \frac{R_R}{\left|Z_R + Z_S\right|^2}. \qquad (2)$$

The total power absorbed in the head was calculated by

$$P_{abs} = \frac{1}{2} \int_V \sigma \left|E\right|^2 dv. \qquad (3)$$

Different negative medium parameters for SAR reduction effectiveness were analyzed. We placed negative permittivity mediums between the antenna and the human head. First, the plasma frequencies of the mediums were set to be $\omega_{pe} = 9.309\times10^9$ rad/s, which give mediums with μ = 1 and ε = -3 at 900 MHz. We set Γ_e = 1.2×10^8 rad/s, suggesting the mediums have losses. The peak SAR 1 gm becomes 1.0697 W/kg with μ = 1 and ε = -3 mediums. Compared to the condition without metamaterials, the radiated power is reduced by 13.9% while the SAR is reduced by 53.43%. With the use of and mediums, the SAR reduction effectiveness is decreased. However, the radiated power from the antenna is less affected. Comparisons of the SAR reduction effectiveness with different positions and sizes of metamaterials were analyzed. Numerical results of SAR value and antenna performance are given in Table 3. In Case 1, the distance between the antenna and metamaterial was changed from 3 to 6 mm. In Case 2, the metamaterial thickness was reduced from 6 to 3 mm. It is found that both the peak SAR 1 g and power absorbed by the head increase with the increase of distance or the decrease of thickness. In Case 3, the size of the metamaterial was increased from 48 × 48 mm to 56 × 56 mm. It can be noted that the peak SAR 1 g is reduced significantly while the dreadful conditions on the radiated power due to metamaterial is insignificant. To further examine whether the metamaterial affected the antenna performance or not, the radiation pattern of the

Table 3. Effects of positions and sizes of metamaterial on antenna performances and SAR values.

Parameter	Z_R (Ω)	P_R (mW)	P_{abs} (mW)	SAR 1 g (W/kg)
Without material	63.39+j94.53	600	268.83	2.002
μ=1, ε=-3	51.43+j99.68	514.6	211.95	1.0697
Case 1	58.37+j95.35	539.4	253.53	1.6105
Case 2	62.19+j96.86	557.2	258.74	1.6893
Case 3	69.15+j107.38	573.33	216.83	1.2346

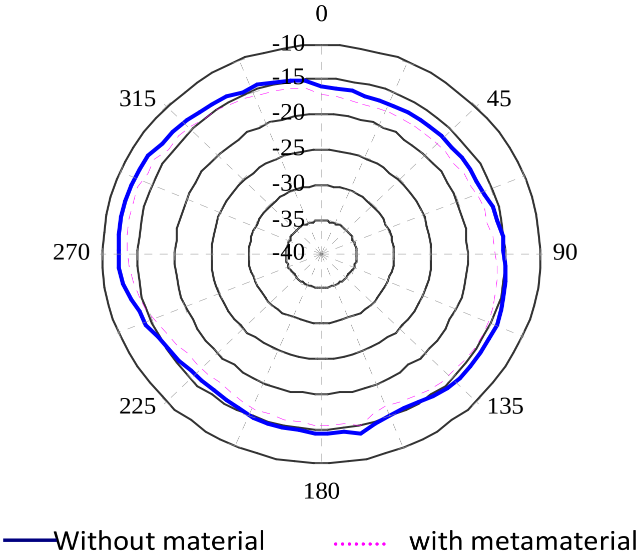

Figure 6. Calculated φ plane radiation pattern at 900 MHz.

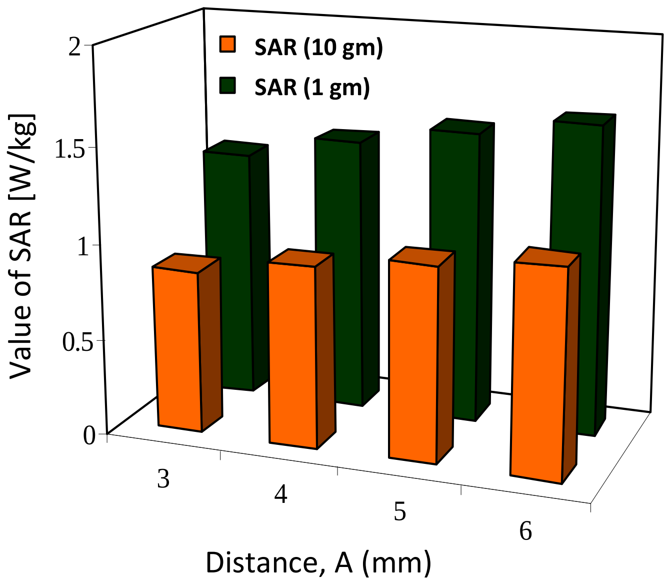

Figure 7. SAR value compared with the distance among antenna and metamaterial.

PIFA antenna with the μ = 1 and ε = -3 metamaterial was analyzed.

The radiation patterns were acquired by the near- and far-field transformation of the Kirchhoff surface integral representation (KSIR) (Ramahi, 1997). All the radiation patterns were normalized to the maximum gain acquired without materials. Figure 6 shows the radiation patterns in φ plane for θ = 90°. In Wang and Fujiwara (1997), the radiation pattern seal to the head is reduced to about 6 dB and our simulation result is similar to their result. With the use of metamaterials, it can be seen that the maximum degradation of the far field does not surpass 1.17 dB.

In Figure 7, it is shown that there is a great influence of the distance among the antenna and metamaterial on SAR diminution. If the distance between the antenna and metamaterial is increased from 3 to 6 mm, then the SAR value also increases from 0.85232 to 1.0734 W/kg for SAR 10 g and 1.3085 to 1.6105 W/kg for SAR 1 g, respectively. This is because the dielectric constant, conductivity, density and magnetic tangent losses conductivity are also varied. In Figure 8, it can be observed that the SAR value increases with the decrease of the thickness of metamaterial. The SAR value reduces quickly when metamaterial size is large 48 × 48 mm to 56 × 56 mm then the SAR value also reduces from 1.0452 to 0.8231 W/kg for the cases of SAR 10 g and 1.5678 to 1.2346 W/kg for SAR 1 g as can be seen from Figure 9.

The use of metamaterials was also compared with other SAR reduction techniques. A PEC reflector and a ferrite material are commonly used in SAR reduction. The PEC reflector and ferrite sheet were analyzed. The relative permittivity and permeability of the ferrite sheet were ε=7.0-j0.58 and μ= 2.83 - j3.25, respectively. Numerical results are shown in Table 4. A PEC placed between the human head and the antenna is studied. It can be found that the peak SAR 1 g is increased with the use of a PEC reflector. This is because the EM wave can be induced in the neighbor of a PEC reflector due to scattering. When the size of PEC sheet is small compared to the human head, the head will absorb more EM energy. Similar results of peak SAR increase with PEC placement were also reported in Hawang and Chen (2006). The use of a ferrite sheet can reduce the peak SAR 1 g effectively. However, the degradation on radiated power from the antenna is also significant. In

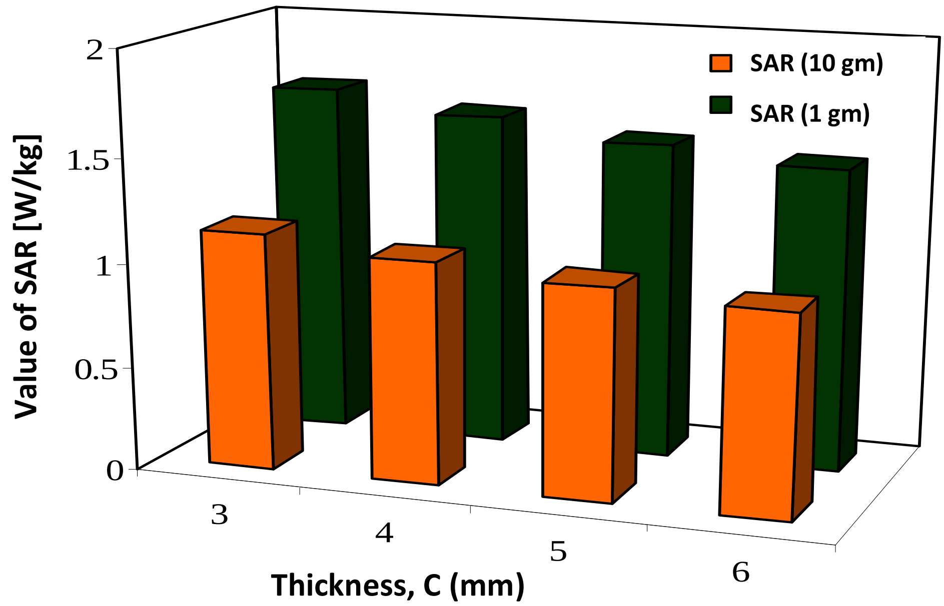

Figure 8. SAR value compared with the thickness of the metamaterial.

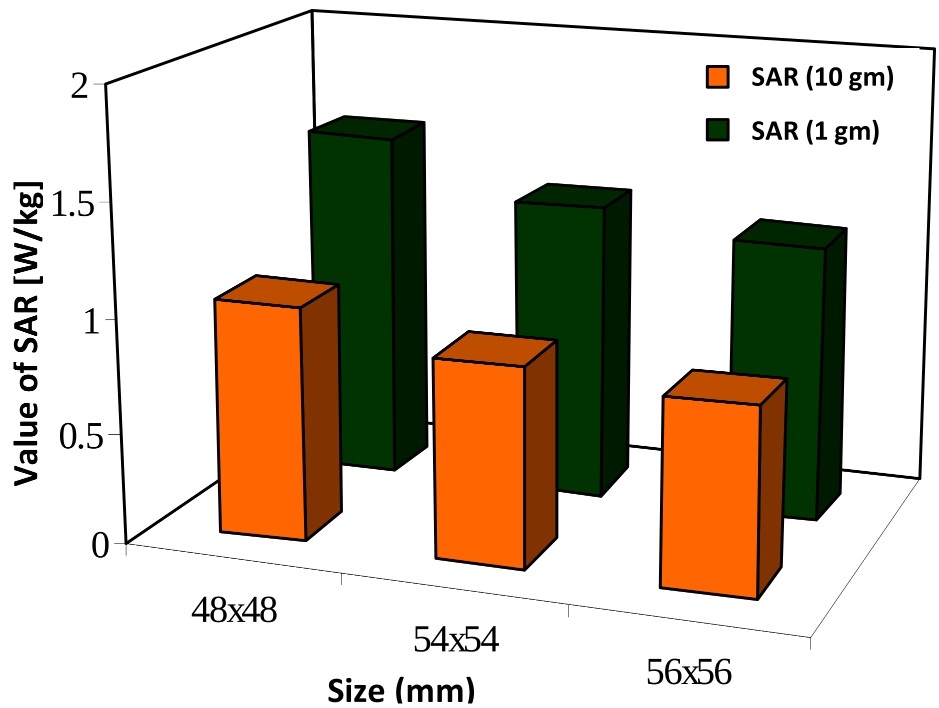

Figure 9. SAR value compared with the size of the metamaterial.

addition, compared to the use of a ferrite sheet, the metamaterials can be designed on the circuit board so they may be easily integrated to the cellular phone.

To study the effect of SAR reduction with the use of metamaterials, the radiated power from the PIFA antenna with μ =1 and ε = -3 mediums was fixed at 600 mW. Numerical results are shown in Table 5. It is found that calculated SAR value at 900 MHz, without the metamaterial, is 2.002 W/kg for SAR 1 g and with the

Table 4. Comparisons of SAR reduction techniques with different materials.

Parameter	Z_R (Ω)	P_R (mW)	SAR 1 gm (W/kg)
μ= 1, $\mathcal{E}$ = -3	51.43+j99.68	514.6	1.0697
PEC reflector	66.83+j32.23	509.3	4.6803
Ferrite sheet	169.33+j153.69	519.3	1.043

Table 5. Effects of comparisons with metamaterials on SAR reduction (P_R = 0.5 W for 900 MHz).

Parameter	900 MHz	
	Without material	μ=1, ϵ =-3
SAR SAR 1 g value for Hawang and Chen (2006)	2.43	1.8
1 g value in this work	2.002	1.16079

metamaterial, the reduction of the SAR 1 g value is 1.16079 W/kg. The reduction is 49.21%.

From simulation results, the metamaterials can reduce peak SAR effectively and the antenna performance can be less affected. The metamaterials are resonant due to internal capacitance and inductance. The mediums will display a stop band with a single negative medium parameter. The propagation constant is imaginary and the fields inside the metamaterials will fall off exponentially with the distance from the surface. This work has achieved 49.21% of SAR reduction where as the design reported in Hawang and Chen (2006) achieved 22.63%, respectively. This is achieved due to the consideration of different density, different antenna, and different size of metamaterial and different type of conductivity.

Conclusion

The EM interaction between an antenna and the human head with materials and metamaterials has been discussed in this paper. Utilizing material in the phone model, a SAR value achieved about 0.676 W/kg for SAR 10 g and with metamaterial, a SAR value of 0.737 W/kg for SAR 10 g is achieved. Based on the 3-D FDTD method with lossy-Drude model, it is found that the peak SAR 1 g of the head can be reduced by placing materials and metamaterials between the antenna and the human head. Metamaterials were designed from a periodic arrangement of SRRS. Numerical results can provide useful information in designing communication equipment for safety compliance.

ACKNOWLEDGEMENTS

The authors would like to thank Institute of Space Science (ANGKASA), Universiti Kebangsaan Malaysia (UKM) and the MOSTI Secretariat, Ministry of Science, Technology and Innovation of Malaysia, e- Science fund: 01-01-02-SF0612, for sponsoring this work.

REFERENCES

Beard BB, Kainz W, Onishi T, Iyama T, Watanabe S, Fujiwara O, Wang J, Bit-Babik G, Faraone A, Wiart J, Christ A, Kuster N, Lee A, Kroeze H, Siegbahn M, Keshvari J, Abrishamkar H, Simon W, Manteuffel D, Nikoloski N (2006). Comparisons of computed mobile phone induced SAR in the SAM phantom to that anatomically corrects model of the human head. IEEE Trans. Electromag. Compatibility, 48(2): 397-407.

Chan KH, Chow KM, Fung LC, Leung SW (2005). Effects of using conductive materials for SAR reduction in mobile phones. Microwave Opt. Technol, Lett., 44(2): 140-144.

Coccioli R, Yang FR, Ma KP, Itoh T (1999). A novel TEM waveguide using uniplanar compact photonic- bandgap (UC-PBG) structure. IEEE Trans. Microw. Theory Tech., 47: 2092–2098.

Curto S, McEvoy P, Bao XL, Ammann MJ (2009). Compact patch antenna for electromagnetic interaction with human tissue at 434 MHz. IEEE Trans. Antenna Propag., 57(9).

Erentok A, Luljak PL, Ziolkowski RW (2005). Characterization of a volumetric metamaterial realization of an artificial magnetic conductor for antenna applications. IEEE Trans. Antennas Propag., 53: 160–172.

Faruque MRI, Islam MT, Misran N (2010a). Effect of human head shapes for mobile phone exposure on electromagnetic absorption, Informacije MIDEM, 40(3): 232-237.

Faruque MRI, Islam MT, Misran N (2010b). Evaluation of specific absorption rate (SAR) reduction for PIFA antenna using Metamaterials, Frequenz J., 64(7-8): 144-149.

Faruque MRI, Islam MT, Misran N (2011a). Analysis of Electromagnetic Absorption in the Mobile Phones Using Metamaterials, Electromag. J. (Taylor & Francis Group). 31 (3): 215-232.

Faruque MRI, Islam MT, Misran N (2011b). Design of handset antenna with low electromagnetic absorption. Austr. J. Basic Appl. Sci., 5 (3): 141-150.

Faruque MRI, Islam MT, Misran N (2011c). Design of metamaterial attachment for SAR reduction in human head, Appl. Comput. Electromag. Soc. J. (ACES J.) 25 (12): 1097-1107.

Faruque MRI, Islam MT, Misran N (2011d). Electromagnetic (EM) absorption reduction in a muscle cube with metamaterial attachment, Med. Eng. Phys. (Elsevier). 33 (5): 646-652.

Faruque MRI, Misran N, Nordin R, Islam MT, Yatim B (2011e). Estimation of Specific Absorption Rate (SAR) and Temperature Increases in the Human Head of Portable Telephones. Scientific Research and Essays (SRE), 6(6): 1209-1215.

Faruque MRI, Misran N, Nordin R, Islam MT, Yatim B (2011f).

Estimation of specific absorption rate (SAR) and temperature increases in the human head of portable telephones, Sci. Res. Essays (SRE). 6(6): 1209-1215.
Fung LC, Leung SW, Chan KH (2002). An investigation of the SAR reduction methods in mobile phone application. IEEE Int. Symp. EMC., 2: 656-660.
Fung LC, Leung SW, Chan KH (2003). Experimental study of SAR reduction on commercial products and shielding materials in mobile phone applications. Microw. Opt. Technol. Lett., 36(6): 419-422.
Hawang JN, Chen FC (2006). Reduction of the peak SAR in the Human Head with Metamaterials. IEEE Trans. Antenna Propag., 54(12): 3763-3770.
Hirata A, Adachi T, Shiozawa T (2004). Folded loop antenna with a reflector for mobile handsets at 2.0 GHz. Microwave Opt. Technol, Lett., 40(4): 272-275.
IEEE C95.1-2005 (2005). IEEE Standards for safety levels with respect to Human Exposure to Radio Frequency Electromagnetic fields,3KHz to 300GHz. Institute of Electrical and Electronics Engineers, Inc. New York.
International Non-Ionizing Radiation Committee of the International Radiation Protection Association (1988). Guidelines on Limits on exposure to radio frequency electromagnetic fields in the frequency range from 100 KHz to 300 GHz. Health Phys., 54(1): 115-123.
Islam MT, Faruque MRI, Misran N (2009). Design analysis of ferrite sheet attachment for SAR reduction in human head. Prog. Electromag. Res., PIER, 98: 191-205.
Islam MT, Faruque MRI, Misran N (2010a). Study of specific absorption rate (SAR) in the human head by metamaterial attachment. IEICE Electron. ExpR., 7(4): 240-246.
Islam MT, Faruque MRI, Misran N (2010b). Specific absorption rate analysis using metal attachment. Informacije MIDEM, 40 (3): 238-240.
Islam MT, Faruque MRI, Misran N (2011a). Electromagnetic (EM) absorption rate reduction of helix antenna with shielding material for mobile phone application. Austr.J. Basic Appl. Sci, 5 (3): 120-133.
Islam MT, Faruque MRI, Misran N (2011b). New low SAR antenna design for mobile handset. Int. J. Phys. Sci. (Accepted), 6 (24): 5706-5715.
Kiminami K, Iyama T, Onishi T, Uebayashi S (2008). Novel specific absorption rate (SAR) estimation method based on 2-D scanned electric fields. IEEE Trans. Electromag. Compatibility, 50(4).
Kiverkas O, Ollikainen J, Lehtiniemi T, Vainikainen P (2004). Bandwidth, SAR, and efficiency of internal mobile phone antennas. IEEE Trans. Electromag. Compatibility, 46(1).
Kuo CM, Kuo CW (2003). SAR distribution and temperature increase in the human head for mobile communication. IEEE-APS Int. Symp. Dig., Columbus, pp. 1025-1028.
Li CH, Chavannes N, Kuster N (2009). Effects of hand phantom on mobile phone antenna performance. IEEE Trans. Antennas Propag., 57(9).
Misran N, Faruque MRI, Islam MT, Abedin HZ (2011). Investigation of dosimetry in human head model for a helical antenna with mobile phone, Int. J. Phys. Sci., 6(5): 1000-1008.
Pedersen GF, Andersen JB (1994). Integrated antennas for hand-held telephones with low absorption. Proc. 44th IEEE Veh. Tech. Conf., Stockholm, Sweden, pp. 1537-1541.
Pendry JB, Holen AJ, Robbins DJ, Stewart WJ (1999). Magnetism from conductors and enhanced nonlinear phenomena. IEEE Trans. Microw. Theory Tech., 47(11): 2075–2084.
Ramahi OM (1997). Near-and far-field calculations in FDTD simulations using Kirchhoff surface integral representation. IEEE Trans. Antennas Propag., 45 (5): 753–759.
Sigalalas MM, Chan CT, Ho KM, Soukoulis (2001). Metallic photonic band gap materials. Phys. Rev. B, 52(16): 11744-11760.
Smith DR, Willie JP, Vier DC, Nemat-Nasser SC, Schultz S (2000). Composite medium with simultaneously negative permeability and permittivity. Phys. Rev. Lett. 84(18): 4184-4187.
Smith DR, Kroll N (2000). Negative refractive index in left handed materials. Phys. Rev. Lett., 85(14): 2933-2936.
Tay RYS, Balzano Q, Kuster N (1998). Dipole configuration with strongly improved radiation efficiency for hand-held transceivers. IEEE Trans. Antennas Propagat., 46(6): 798-806.
Wang J, Fujiwara O (1997). Reduction of electromagnetic absorption in the human head for portable telephones by a ferrite sheet attachment. IEICE Trans. Commun. E80b (12): 1810-1815.
Wang J, Fujiwara O (1999). FDTD computation of temperature rise in the human head for portable telephones. IEEE Trans. Microwave Theory Tech., 47(8): 1528-1534.
Ziolkowski RW (2003). Design, fabrication, and testing of double negative metamaterials. IEEE Trans. Antennas Propag., 51(7): 1516–1529.